River Flow 2010 - Dittrich, Koll, Aberle & Geisenhainer (eds) - © 2010 Bundesanstalt für Wasserbau ISBN 978-3-939230-00-7

Scour and dune morphology in presence of large wood debris accumulation at bridge pier

S. Pagliara & I. Carnacina
Civil Engineering Department, University of Pisa, Via Gabba 22, 56122, Pisa, Italy

ABSTRACT: The presence of debris accumulation on bridge pier scour increases the bridge failures likelihood, accelerating the scour development and increasing the maximum scour hole depth. Likewise, the scour morphology is substantially modified by the flow interaction with the debris accumulation and the bridge pier. The paper aims to analyze the effect of the debris accumulation on both scour hole and morphology at high evolution stages. Experimental tests have been carried out at the PITLAB hydraulic centre of the Civil Engineering department of the University of Pisa, Pisa, Italy. Tests have been performed in several debris geometries, flow contractions, and hydraulic conditions, in order to cover a wide parameters range. Different debris shapes, longitudinal lengths and longitudinal extensions downstream to the pier centre have been tested. Scour morphologies have been analyzed both in terms of maximum longitudinal and transversal length respect to tests without accumulation. As well, the dune evolution in respect to the main parameters, (flow intensity and shallowness) has been analyzed. As results, a simple equation to predict the maximum scour morphology will be developed, together with new analytical equation to predict maximum scour depth and longitudinal and transversal lengths.

Keywords: Bridge scour, Debris accumulation, Scour morphology, Dune

1 INTRODUCTION

This paper aims to analyze the effect of debris accumulations at bridge piers on scour and dune temporal evolutions and the dune morphologies, compared to those of an isolated cylindrical pier under same hydraulics and sediment conditions. Debris accumulations at bridge piers and decks have been mainly divided into two classes (Bradley et al., 2005): single pier debris accumulations and span-blockage accumulations. In the present study only isolated or single pier accumulations have been analyzed for the sake of simplicity.

Indeed, it is well known that several variables affect the scour evolution and the maximum equilibrium clear-water scour hole depth for isolated pier in uniform sediment, i.e., flow shallowness h/D, where h = water depth D = pier diameter, flow intensity U/U_c, where U = average flow velocity and U_c = sediment threshold flow velocity, sediment coarseness D/d_{50}, where d_{50} = sediment diameter for which 50% in weight is finer, and non-dimensional time $T = Ut/h$, where t = time (Melville and Sutherland, 1988; Franzetti et al., 1989; Franzetti et al., 1994). As well, the pier Froude number U^2/gD, where g = gravitational acceleration, should be taken into account to achieve a correct flow similitude. However, piers Froude numbers are higher in laboratory experiences than in field experiences. Hence, equations developed for flumes are quite conservative and tends to overestimate the prototype maximum scour hole depth z_{max}/D, where z_{max} = maximum scour hole measured at the bridge pier (Ettema et al., 1998). Alternatively, Oliveto and Hager (2002), based their analysis on the hydraulic resistance analogy, in which z_{max}/D depended on a non dimensional time parameter and on the densimetric Froude number $F_d=U/(g'd_{50})$, where $g' = g(\rho_s-\rho)/\rho$ = reduced gravitational acceleration (Dey and Debnath, 2001; Oliveto and Hager, 2002; Dey and Raikar, 2005), ρ_s = sediment density and ρ = water density.

The presence of debris or drift accumulations further complicates the scour process in correspondence of bridge piers. The debris build-up causes: a contraction, reducing the waterway width; a local scour increase, due to the accumulation obstruction; a deflection of the flow angle of attack, which can increase the local scour around

the bridge; and, finally, a reduction of the bridge discharge capacity (Kattell and Eriksson, 1998).

Recently, several experimental studies and field observations have been carried out to asses the effect of smooth or rough debris accumulation on z_{max}/D (Melville and Dongol, 1992; Diehl, 1997; Kattell and Eriksson, 1998; Parola et al., 2000; Richardson and Davis, 2001; Bradley, Richards et al., 2005; Briaud et al., 2006; Zevenbergen et al., 2006; Lagasse et al., 2009; Pagliara and Carnacina, 2010).

Specifically, Melville and Dongol (1992) made tests using a cylindrical accumulation extending downstream of the bridge pier. They defined an equivalent bridge pier diameter D_e based on flow and accumulation geometric characteristics, i.e., t_d = debris thickness and d_d = debris diameter

$$D_e = \left[0.52 t_d d_d + \left(h - 0.52 t_d\right)\right] / h \quad (1)$$

Later on, Lagasse et al. (2009) developed a similar approach defining a D_e based on accumulation shape and plunging flow factors for flume tests, including several debris accumulation shapes, geometry and roughness. Lastly, Pagliara and Carnacina (2010), studied the temporal scour evolution for accumulation with different roughness, porosity, and percentage rough blockage ratio $\Delta A = [(d_d - D)\cdot(t_d + d_f)]/(b\cdot h)\cdot 100 = \Delta A$ for $d_f = 0$, in which d_f = average logs diameter and b = channel width, from which it can be inferred that the porosity slightly effect the scour evolution, whilst both ΔA and roughness play an important role on z_{max}/D temporal evolution. In particular:

$$z_{max}/D = \xi \ln\left(T^*/10\right) \quad (2)$$

in which

$$\xi = 0.19\left(U/U_c \Delta \tilde{A}^{0.4}\right) - 0.13 \quad (3)$$

where ξ = non-dimensional time parameter, $T^* = hUt/A_{acc}$ = non-dimensional blockage dependent time, $A_{acc} = (d_d - D)t_d + hD$ = additional area occluded by the accumulation.

However, little is known on scour and dune morphologies in presence of debris accumulation and their maximum width and length, which are of main importance in order to efficiently design pier protection structures.

2 EXPERIMENTAL APPARATUS

2.1 *Flume characteristics*

All experimental runs were carried out at the PIT-LAB research center of the Civil Engineering Department of the University of Pisa, Italy. The channel consisted of a glass walled horizontal flume 12 m long, 0.61 m wide and 0.5 m deep. The flow was supplied by means of a sluice gate provided with a flow straightener (0.25 cm mesh).

The discharge was measured by means of a KRONE® electromagnetic gauge, installed in the supply line. A false bottom 2 m long, 0.15 m deep, and 0.6 m wide was used to simulate the scoured zone. An upstream steel box 3 m long, 0.6 m wide and 0.15 m deep provided the transition between the scoured zone and the inlet sluice gate. A Downstream second box 1 m long, 0.6 m wide and 0.15 m deep, closed the false bottom. One perspex cylindrical pier of diameter D=0.03 m has been used in the tests. The pier was placed at the false bottom center. A weir, positioned 2 m downstream from the last box, regulated the water depth.

A ultrasonic Baumer® UNDK20 transducer mounted on a point gauge 0.1 mm precise and a Gefran® MK4 distance meter connected to the trolley mechanism have been used to survey the final maximum scour profile and the liquid profile. During the test execution, scour measurements near the pier z_{max} were taken at t=1, 2, 4, 8, 15, 30, 60…, 360 …minutes. The tests were generally performed for 360 minutes, whilst several tests have been lasted up to 96 hour. z_{max} has been measured by means of a clear scale glued at the pier surface. Its use prevent from any disturbance effect which may occur when measuring z_{max} with intrusive techniques, i.e., point gauge.

2.2 *Large wood debris and sediment features*

In the present study, tests have been carried out with frontal rectangular large wood debris (LWD) accumulations, though several others shapes are known in literature, i.e., cylindrical (Melville and Dongol, 1992), or triangular (Zevenbergen et al., 2006).

Table 1. Tested LWD accumulations

Test series	l_d/D	d_d/D	l_d/d_d	t_d/d_d	p_d/l_d	
EB	3	10	0.05	0.01	0.5	min
	6	20	0.10	0.39		max
E	2.50	3.10	0.44	0.18	0	min
	3.60	6.90	0.65	1.2		max

Table 1 reports the LWD (large wood debris) geometric characteristics tested in the present study. In the table, l_d = LWD streamwise length and p_d = distance between the debris downstream edge and the pier center (fig. 1a). In the present study, LWD were simulated by means of synthetic material, modeled in order to obtain a rectangular cross-sectional shape (fig 1b). Two different tests

series have been carried out, i.e., the "EB" test series, which is characterized by wider accumulations centered respect to the pier center, and "E" test series, which were characterized by narrower accumulation which never extended downstream the bridge pier center.

Figure 1a-c depicts the experimental sketch and notation, where, z_{max}= maximum scour depth near the pier, and z_M = maximum dune height.

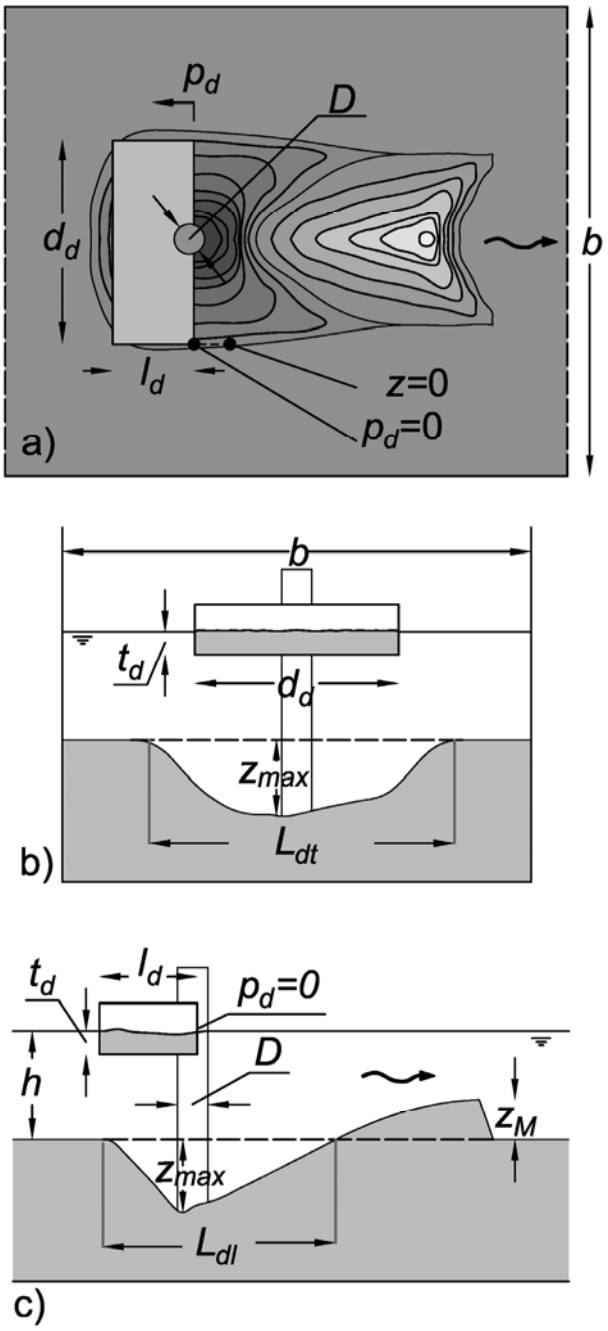

Figure 1. Sketch and notation: a) plan view, b) transverse section and c) longitudinal section.

Medium river sand has been used for all the tests, whose granulometric characteristics are: d_{50}= 1 mm, σ=$(d_{84}/d_{16})^{0.5}$ = 1.2 = standard deviation of sediments, φ = 31° and φ' = 36° are the dry and wet sediment angles of repose, and ρ_s = 2440 daN/m^3. The critical velocity U_c has been evaluated according to Pagliara and Carnacina (2010), in which the critical Shields parameter Θ_c=0.032.

2.3 *Experimental range*

Before each experiment, the bed was carefully leveled around the bridge pier and the LWD was fixed at different distances from the bed, to obtain different t_d values. Hence, the channel was completely filled up with water at low discharge. The discharge Q was regulated to the test's discharge and time measurement started after adjusting the water elevation. Details on the tests execution are available in Pagliara and Carnacina (2010). Table 2 reports the flow conditions tested in the present study for both tests series, where $F_r = U/(gh)^{0.5}$ = Froude number and $R_e = 4Uh/v$ = Reynolds number, in which v = kinematics viscosity.

Table 2. Experimental tested conditions

Test series	U [m/s]	U/U_c	h/D	ΔA	F_r	F_d	$R_e \cdot 10^{-4}$	
EB	0.16	0.5	2.66	0	0.12	1.33	5.48	min
	0.35	1	5.66	50	0.40	2.95	22.2	max
E	0.21	0.67	2.66	0	0.16	1.77	7.7	min
	0.35	1	5.66	13	0.40	2.95	22.2	max

3 RESULTS AND DISCUSSION

Figures 2a-h show top views of the final dry scour (6 hours) with different dune morphologies observed at various flow and blockage conditions.

In the right, the plot shows the contour lines with the scour values observed for the tests. The longitudinal x axis and the transversal y axis relates to the pier center, whilst the vertical elevation measured with the ultrasonic transducer Z relates to the original bed elevation. As shown in the figure, the debris accumulation significantly affects the scour morphology. The dune, in clear water condition, is composed by the material scoured near the pier. As observed by (Mazumder et al., 2009) the dune presence generates high turbulence disturbance which, hence, is responsible of the secondary erosion process immediately downstream of the dune itself. Moreover, for low U/U_c, as far as ΔA increases, the scour increases its width and a multiple dune develops downstream the pier (fig. 2c, d, i, and k). Vice versa, even at high U/U_c, but for low ΔA, the dune presents a typical swallow-tail shape, which can be observed also in case of isolated pier (fig. 2a, b, e, f, g, h). Therefore, both z_{max}/D and z_M/D temporal evolution have been analyzed in order to isolate different scour and dune morphologies. Figure 3 shows z_{max}/D temporal scour evolution for both "E" and "EB" tests series, i.e., for

$0<\Delta A<50$ and $2.66<h/D<5.66$. Accordingly, as observed by Pagliara and Carnacina (2010), z_{max}/D shows an almost linear dependence in the semi-log chart on T^*, where the x-axis intercept has been fixed equals to $T^*=10$. As also observed by Melville and Dongol (1992), when $\Delta A>0$ and for $U/U_c=1$, z_{max}/D could shows values up to 4 times D.

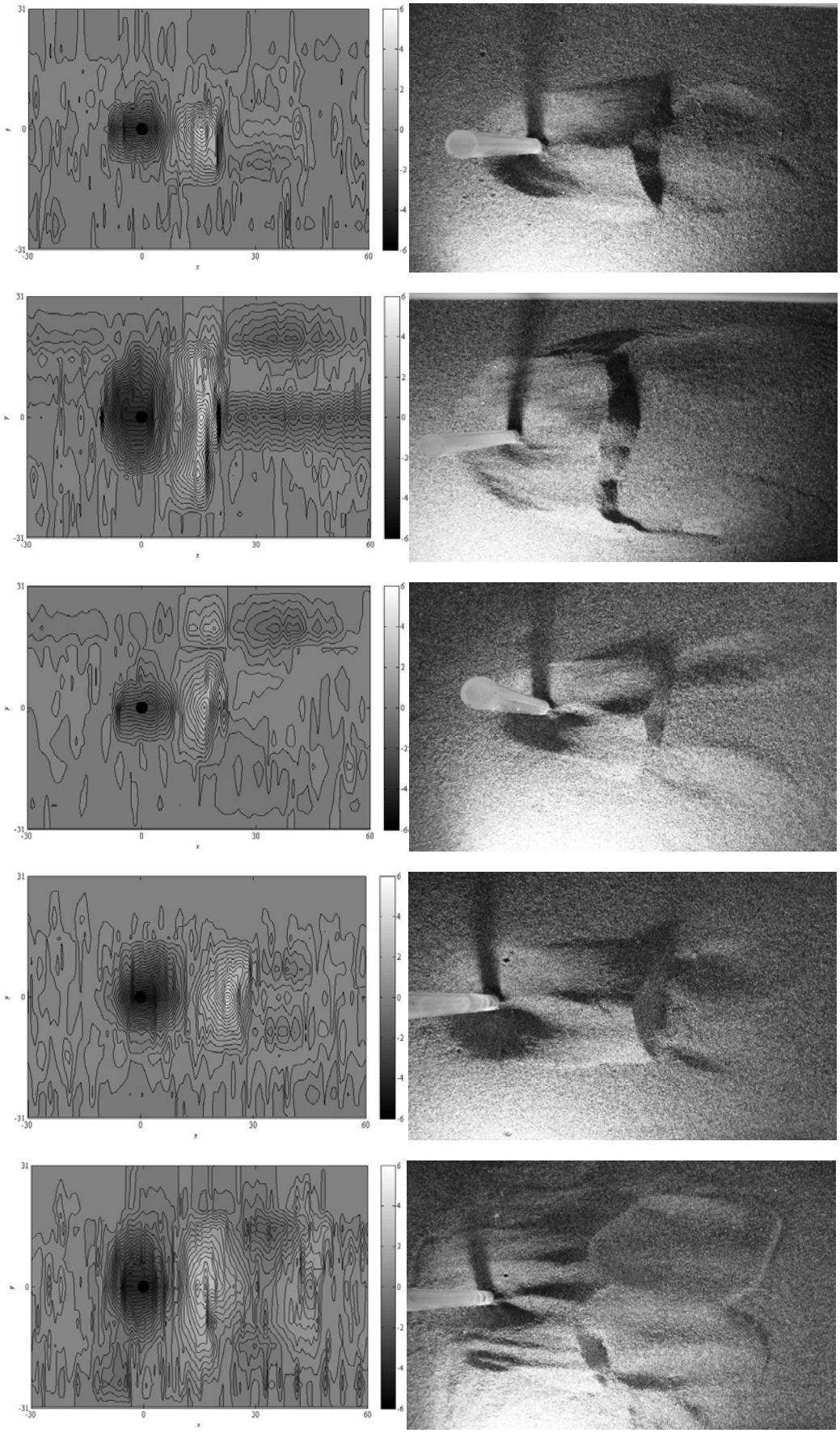

Figure 2. Dune morphologies for test a, b) EB18, c. d) EB20, e. f) EB21, g, h) EB50 and i, k) EB53 (x, y and Z axes in cm).

Vice versa, the dune evolution shows a totally different dependence on T^*. In fact, at U/U_c=1, as shown by the dotted line in fig. 4a, z_M/D first shows a maximum at $10^2<T^*<10^4$ with values ranging $0.6<z_M/D<1.7$, whilst for higher T^*, z_M/D strongly reduced.

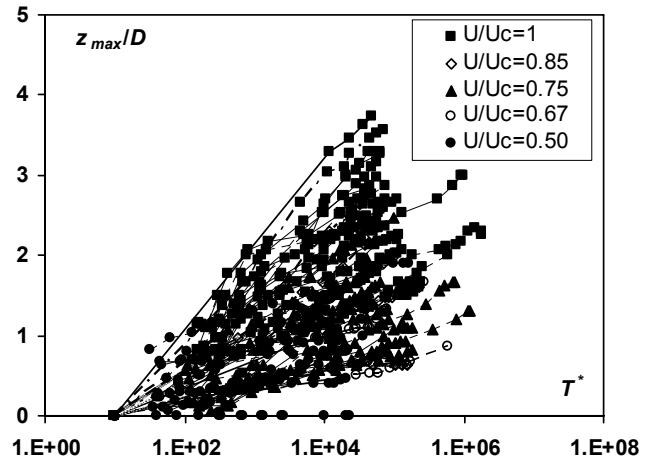

Figure 3. z_{max}/D vs. T^* for $0<\Delta A<50$ and $2.66<h/D<5.66$.

For $0.5<U/U_c<0.75$, z_M/D again shows a behavior which is comparable to that of the maximum scour, in which z_M/D increases within T^* (fig. 4b), though, showing values comparable to the maximum z_M/D observed for U/U_c=1.

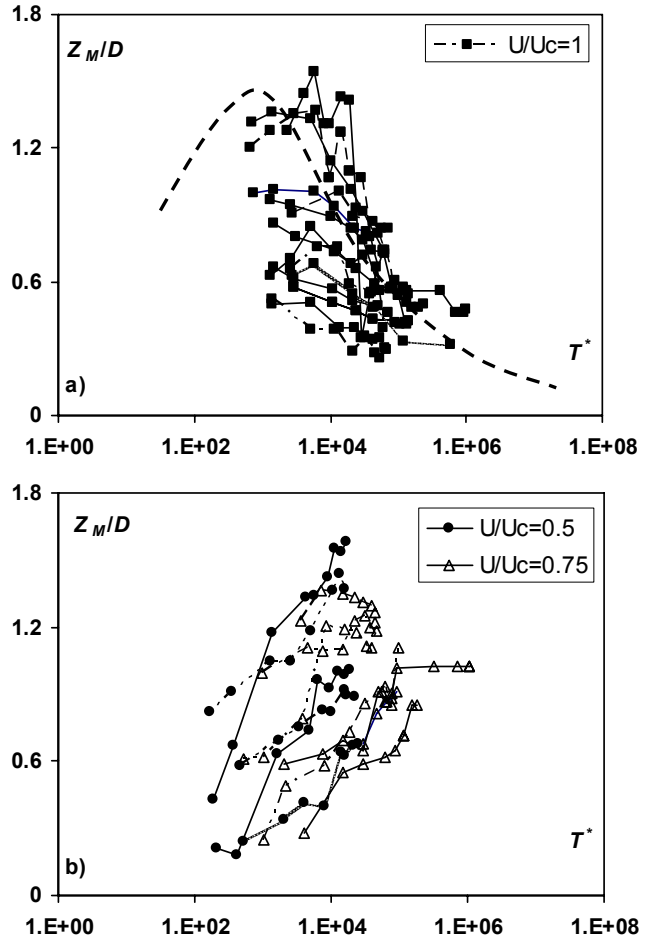

Figure 4. z_M/D vs. T^* for $0<\Delta A<50$ and $2.66<h/D<5.66$, a) eroded dunes, and b) stable dunes.

Based on the visual observation and on the z_M/D temporal evolution analysis, three different dune morphologies have been distinguished in fig. 5, i.e., eroded single dune (N_{SD}), stable single dune (S_{SD}), and stable multiple dune (S_{MD}). N_{SD} is characterized by the continuous removal of sediment from the dune, typically presenting the dune temporal evolution observed in fig. 3.

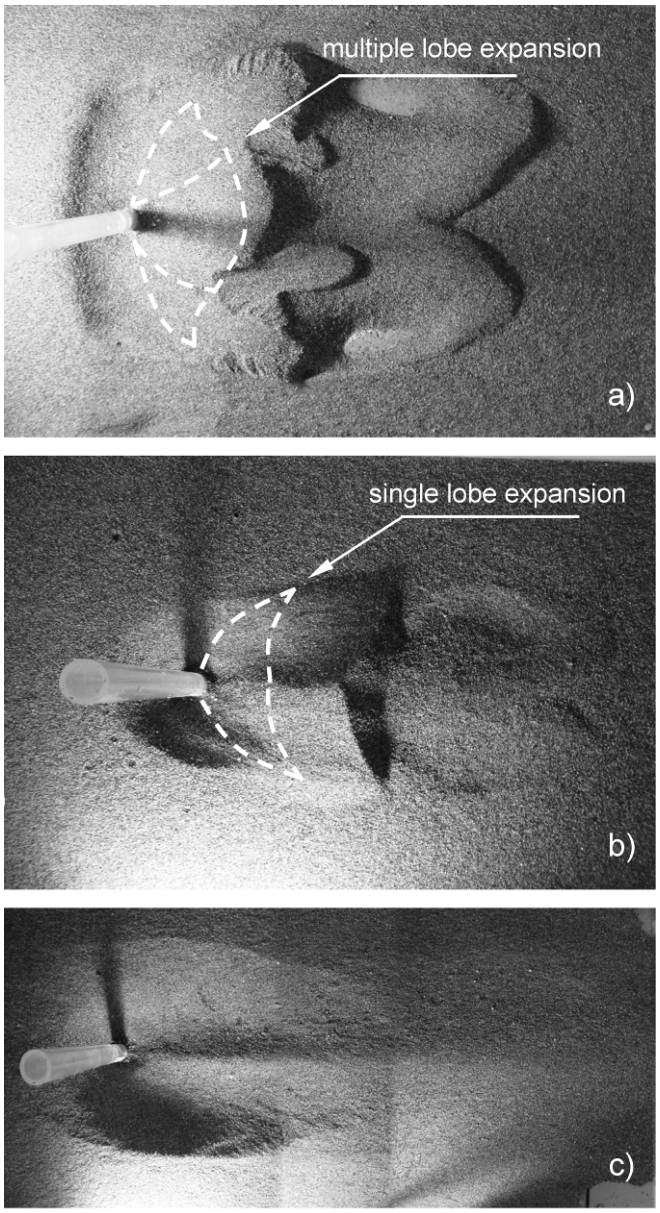

Figure 5. Observed dune morphologies: a) stable multiple dunes, S_{MD}, b) stable single dune, S_{SD} and c) eroded single dune N_{SD}.

The dune continuously propagates downstream until the original swallow-tail shape cannot be distinguished. Sediments are continuously removed from the downstream scour side and the scour hole showed an elongated shape, while the dune is smashed down by the flow turbulence. As for either ΔA or U/U_c where reduced, the dune slowly propagates downstream and S_{SD} morphology was distinguished. As shown by fig. 5b, S_{SD} presented a single lobe expansion, in which the dune front was featured by a swallow-tail shape. In the tested

range, z_M/D present either increasing dependence with T^*, or, after a developing phase, could reach a plateau, after which the dune only translate downstream. Sediments were removed from the scour hole and accumulated downstream. As observed, a secondary scour could be generated downstream of the dune. Finally, the S_{MD} morphology was distinguished at low U/U_c and high ΔA. It showed a slow multiple lobe propagation, in which the dune was featured by multiple fronts which expanded along all the channel width. Hence, each test has been classified in terms of U/U_c and ΔA in fig. 6, for h/D=2.66 (empty symbol) and h/D=5.66 (filled symbol). The figure also shows non scoured tests. The solid line in the upper part of the plot distinguished the transition between the localized scour and the global scour, which have been distinguished from preliminary tests in which sediments were scoured, from the channels sides, from the beginning up to the tests end.

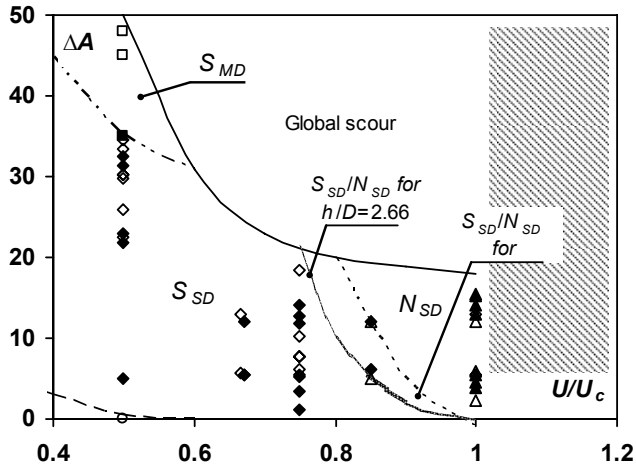

Figure 6. Dune morphology classification in presence of debris occlusion: no scour (h/D=2.66 ○, h/D=5.66 ●), S_{SD} (h/D=2.66 □, h/D=5.66 ■), N_{SD} (h/D=2.66 ◇, h/D=5.66 ◆) and S_{SD} (h/D=2.66 △, h/D=5.66 ▲).

The hatched region shows the sediment transport threshold, after which bed-forms develop and for which the dune classification is no longer valid. Indeed, after the threshold condition, the effect of the upstream sediment movement may change both the scour morphology and the scour pattern (Melville, 1984) and the dune morphology. It is worth noticing that for h/D=2.66 the transition from S_{SD} to N_{SD} is drawn down toward ΔA. In fact, the effect of the surface wake downstream of the accumulation increases the turbulence toward the bed, contributing to higher dune erosions even at lower U/U_c. Differently, for U/U_c=0.5, the transition from S_{MD} to S_{MD} slightly differs for 2.66<h/D<5.66, and a single transition has been identified. Results also agree with (Melville and Coleman, 2000), who observed the scour formation, for ΔA=0, at 0.3<U/U_c<0.5.

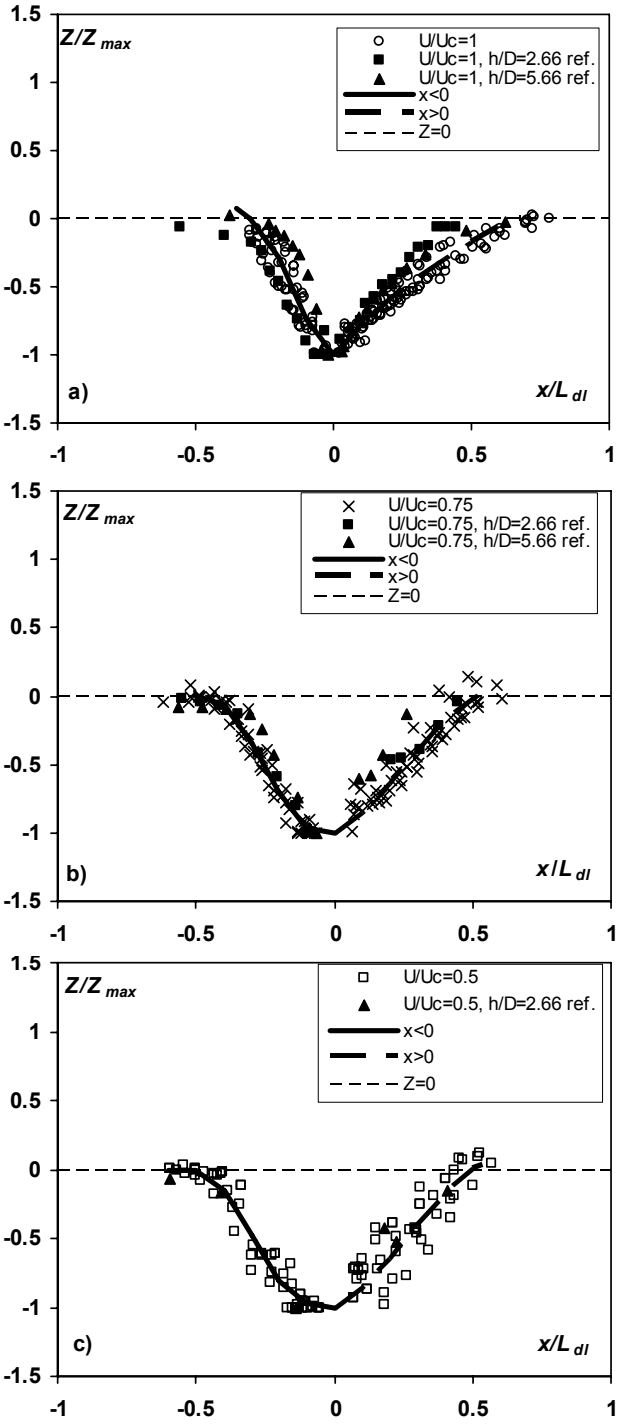

Figure 7. Self-similar non-dimensional longitudinal scour for for 0<ΔA<50 and 2.66<h/D<5.66.

Hence, both longitudinal and transverse scour profiles have been thorough analysed. Figures 7a-c shows the non-dimensional maximum scour hole longitudinal sections normalized by L_{dl} for 0.5<U/U_c<1, 0<ΔA<50, and 2.66<h/D<5.66, where Z = scour depth and Z_{max} is the maximum scour hole, both measured with the ultrasonic sensor. Accordingly, as U/U_c increases, the scour hole propagates downstream, for the dune erosive action showed at higher U/U_c. Indeed, as U/U_c approaches the lowest values, L_{dl} equally distributed in both the downstream and the upstream sides, as the dune steepness affects the sediment

transport and contributes to the reduce the sediment removal from the groove. As well as for L_{dl}, the maximum scour shift downstream as far as U/U_c increases. Reference tests with ΔA=0 are, generally, lesser extended downstream, as for the flow contraction, generated by the debris accumulation, showed a higher erosive action on the downstream side of the scour hole.

Normalised scour profiles can be approximated by polynomial functions, i.e., for x<0:

$$Z/Z_{max} = a\left(x/L_{dl}\right)^5 + b\left(x/L_{dl}\right)^4 + \\ +c\left(x/L_{dl}\right)^3 + d\left(x/L_{dl}\right)^2 + e\left(x/L_{dl}\right) - 1 \quad (3)$$

whilst for x>0:

$$Z/Z_{max} = \alpha\left(x/L_{dl}\right)^3 + \beta\left(x/L_{dl}\right)^2 + \\ +\gamma\left(x/L_{dl}\right) - 1 \quad (4)$$

Where a-e and α-γ are regressions coefficients which depended on U/U_c (table 3).

Table 3. Eq.3-4 Normalised scour hole coefficients

Eq. Coefficients	U/U_c		
	1	0.75	0.5
a	1105	88.25	-160
b	1190	103.1	-241
c	492.7	16.01	-109.2
d	90	12.87	-11.53
e	2.5	1.05	-0.59
α	-0.014	-7.23	-6.51
β	-1.04	5.6	5.32
γ	2.8	0.93	0.97

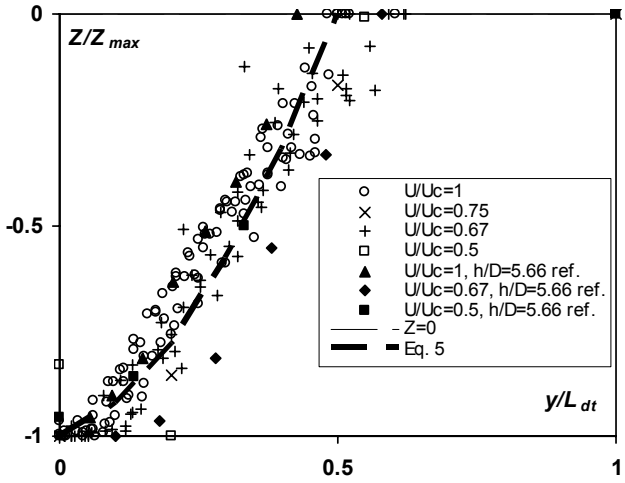

Figure 8. Self-similar non-dimensional transverse scour for 0<ΔA<30 and 2.66<h/D<5.66.

Normalized scour hole profiles show a good similarity in terms of U/U_c, especially for x<0, whilst for x>0 the profile slightly scatters. Slight scatter toward eq.4-5 is likely connected to the effect of neglected variables, such as ΔA, h/D and accumulation shape and l_d, which, however, showed a slight influence on the scour hole longitudinal morphologies.

Figure 8 shows the self-similar transverse profile normalized by L_{dt}, for 0<ΔA<30 and 2.66<h/D<5.66. Unlike the longitudinal profiles, the transverse ones are less affected by U/U_c.

Hence, normalized scour profiles have been approximated by eq.5:

$$Z/Z_{max} = 3\left(y/L_{dt}\right)^2 + 0.5\left(y/L_{dt}\right) - 1 \quad (5)$$

in which the Z/Z_{max}=0 for y/L_{dt}=0.5. Scour maximum hole position in transverse direction lays generally between 0<y/L_{dt}<0.2.

In order to highlight the differences between scour width and length, two debris influence coefficients have been defined, i.e., $K_l = L_{dl}/L_{dl\text{-}o}$ = longitudinal scour debris accumulation coefficient, and $K_t = L_{dt}/L_{dt\text{-}o}$ = transverse scour debris accumulation coefficient, where the suffix $-o$ identifies tests with ΔA=0, i.e., without accumulation. Both coefficients were evaluated for T^*=10^4, after which the effect of time was found almost negligible.

Figures 10 and 11 show the dependence of K_l and K_t on both ΔA and U/U_c for 2.66<h/D<5.66 and both "EB" and "E" test series. Accordingly, as the effect of ΔA became more relevant, the scour hole increases its length and width, as well as, given constant ΔA, K_l and K_t increased with U/U_c, up to 3 times the scour hole without accumulation.

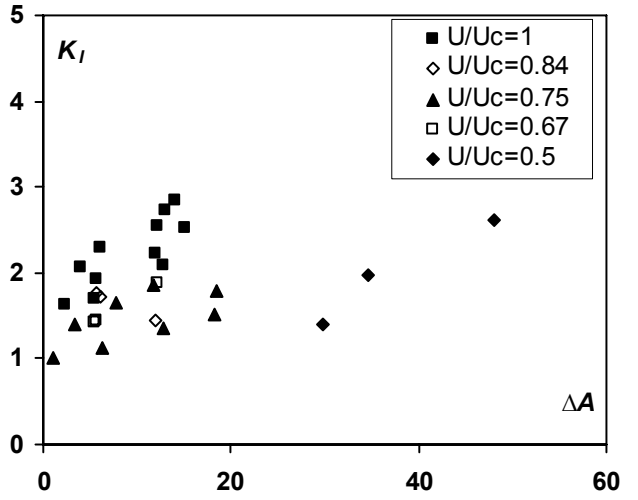

Figure 10. Influence of ΔA and U/U_c on K_l for 2.66<h/D<5.66.

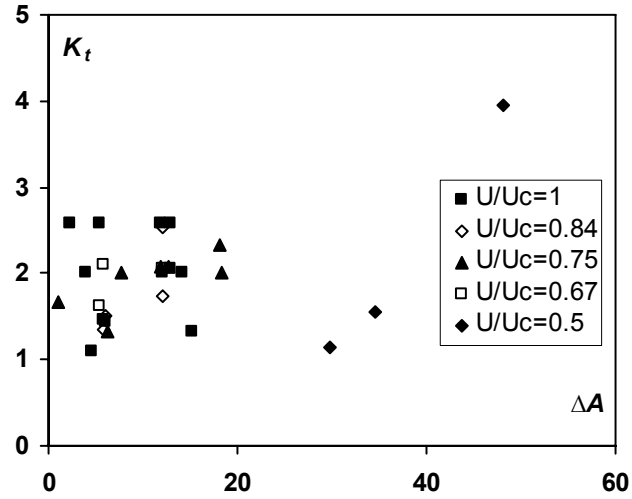

Figure 12. Influence of ΔA and U/U_c on K_t for $2.66<h/D<5.66$.

Note that for $\Delta A>40$, scour width could eventually show values 3.9 times the scour without accumulation. These results agree with the patterns observed for S_{MD}, which generally presented larger values compared to that observed for S_{SD} or N_{SD}.

Both K_l and K_t can be approximated by eq. 6:

$$K_l = \left(0.2U/U_c - 0.09\right)\Delta A + 1 \quad (6)$$

and eq. 7 respectively

$$K_t = \left(0.2U/U_c - 0.077\right)\Delta A + 1 \quad (7)$$

for which K_l=1and K_t=1 as ΔA=0.

4 CONCLUSIONS

Scour and dune morphologies in presence of several debris accumulations at bridge pier in clear water condition have been analyzed. The debris accumulation deeply affect both maximum scour hole depth, length, width and dune morphology, leading to dangerous effect on the bridge pier stability

The temporal analysis of z_M demonstrated that the dune could be eroded under given condition of high occlusion or high flow intensity. Therefore, tree main dunes morphologies have been distinguished in clear water conditions, i.e., eroded and stable single dune and stable multiple dunes. Both scour longitudinal and transverse maximum scour morphologies have been analyzed, showing a strong self-similar pattern when normalized by maximum L_{dl} and L_{dt} respectively. Finally, maximum scour length and width showed, respectively, values up to 3 and 4 times that without debris accumulation.

REFERENCES

Bradley, J. B., Richards, D. L., Bahner, C. D. 2005. Debris Control Structures Evaluation and Countermeasures, FHWA-IF-04-016 Hydraulic Engineering Circular No. 9, U.S. Department of Transportation, F.H.A., Washington, D.C.

Briaud, J. L., Chen, H. C., Chang, K. A., Chen, X., Oh, S. J. 2006. Scour at bridges due to debris accumulation: A review. 3rd International Conference on Scour erosion. Amsterdam, The Nederland: CD-ROM.

Dey, S., Debnath, K. 2001. Sediment pickup on streamwise sloping beds. Journal of Irrigation and Drainage Engineering-Asce, 127(1), 39-43.

Dey, S., Raikar, R. V. 2005. Scour in long contractions. Journal of Hydraulic Engineering, 131(12), 1036-1049.

Diehl, T. H. 1997. Potential drift accumulation at bridges, FHWA-RD-97-028, Federal Highway Administration, Washington, D.C.

Ettema, R., Melville, B. W., Barkdoll, B. 1998. Scale effect in pier-scour experiments. Journal of Hydraulic Engineering-Asce, 124(6), 639-642.

Franzetti, S., Larcan, E., Mignosa, P. 1989. Erosione alla base di pile circolari di ponte:verifica sperimentale dell'ipotesi di esistenza di una situazione finale di equilibrio. Idrotecnica, 3, 135-139.

Franzetti, S., Malavasi, S., Piccinin, C. 1994. Sull'erosione alla base delle pile dei ponti. XXIV Convegno d'idraulica e costruzioni idrauliche. Naples. Italy.

Kattell, J., Eriksson, M. 1998. Bridge Scour Evaluation: Screening, Analysis, & Countermeasures, 9877 1207—SDTDC, Service, U.F., San Dimas Technology and Development Center, San Dimas, California.

Lagasse, P. F., Clopper, P. E., Zevenbergen, L. W. 2009. Impacts of debris on bridge pier scour. 33rd IAHR Congress. Vancouver: 3967-3974.

Mazumder, B. S., Pal, D. K., Ghoshal, K., Ojha, S. P. 2009. Turbulence statistics of flow over isolated scalene and isosceles. Journal of Hydraulic Research, 47(5), 626-637.

Melville, B. W. 1984. Live-Bed Scour at Bridge Piers. Journal of Hydraulic Engineering-Asce, 110(9), 1234-1247.

Melville, B. W., Coleman, S. E. 2000. Bridge Scour. Highlands Ranch, Colorado, Water Resources Publications, LLC.

Melville, B. W., Dongol, D. M. 1992. Bridge Pier Scour with Debris Accumulation. Journal of Hydraulic Engineering-Asce, 118(9), 1306-1310.

Melville, B. W., Sutherland, A. J. 1988. Design Method for Local Scour at Bridge Piers. Journal of Hydraulic Engineering-Asce, 114(10), 1210-1226.

Oliveto, G., Hager, W. H. 2002. Temporal evolution of clear-water pier and abutment scour. Journal of Hydraulic Engineering-Asce, 128(9), 811-820.

Pagliara, S., Carnacina, I. 2010. Temporal scour evolution at bridge piers: Effect of wood debris roughness and porosity. Journal of Hydraulic Research, 48(1), 3-13.

Parola, A. C., Apelt, C. J., Jempson, M. A. 2000. Debris forces on highway bridges. Transportation Research Record, NCHRP Report No. 445, Transportation Research Board, Washington, D.C.

Richardson, A., Davis, S. R. 2001. Evaluating Scour At Bridges, HEC18, U.S. Departement of Transportation, F.H.A.

Zevenbergen, L. W., Lagasse, P. F., Clopper P.E., Spitz, W. J. 2006. Effects of debris on bridge pier scour. 3rd International conference on scour and erosion. Amsterdam, The Netherlands.